We are IntechOpen,
the world's leading publisher of
Open Access books
Built by scientists, for scientists

6,900
Open access books available

186,000
International authors and editors

200M
Downloads

Our authors are among the

154
Countries delivered to

TOP 1%
most cited scientists

12.2%
Contributors from top 500 universities

Interested in publishing with us?
Contact book.department@intechopen.com

Numbers displayed above are based on latest data collected.
For more information visit www.intechopen.com

Free Vibration Analysis of Spinning Spindles: A Calibrated Dynamic Stiffness Matrix Method

Seyed M. Hashemi and Omar Gaber

Additional information is available at the end of the chapter

1. Introduction

The booming aerospace industry and high levels of competition has forced companies to constantly look for ways to optimize their machining processes. Cycle time, which is the time it takes to machine a certain part, has been a major concern at various Industries dealing with manufacturing of airframe parts and subassemblies. When trying to machine a part as quick as possible, spindle speed or metal removal rates are no longer the limiting factor; it is the chatter that occurs during the machining process. Chatter is defined as self-excited vibrations between the tool and the work piece. A tight surface tolerance is usually required of a machined part. These self-excited vibrations leave wave patterns inscribed on the part and threaten to ruin it, as its surface tolerances are not met. Money lost due to the destructive nature of chatter, ruining the tools, parts and possibly the machine, has driven a lot of research into determining mathematical equations for the modeling and prediction of chatter. It is well established that chatter is directly linked to the natural frequency of the cutting system, which includes the spindle, shaft, tool and hold combination.

The first mention of chatter can be credited to Taylor [18], but it wasn't until 1946 that Arnold [3] conducted the first comprehensive investigation into it. His experiments were conducted on the turning process. He theorized that the machine could be modelled as a simple oscillator, and that the force on the tool decreased as the speed of the tool increased with relation to the work piece. In his equations, the proportionality constant of the speed of the tool to the force was subtracted from the damping value of the machine; when the proportionality constant increases beyond the damping value of the machine, negative damping occurs causing chatter. This was later challenged by Gurney and Tobias who theorized the now widely accepted belief that chatter is caused by wave patterns traced onto the surface

of the work piece by preceding tool passes [9]. The phase shift of the preceding wave to the wave currently being traced determines whether there is any amplification in the tool head movement. If there exists a phase shift between the two tool passes, then the uncut chip cross-sectional area is varied over the pass. The cutting force is dependent on the chips cross sectional area, and so, a varying cutting force is produced [19]. To perform calculations on this system, they modelled a grinding machine as a mass-spring system as opposed to an oscillating system. It had a single degree of freedom, making its calculations quite simple. The spring-mass system is also the widely used modelling theory for how a vibrating tool should be characterized today.

Prior to 1961, the research papers published on the machining processes regarded them as steady state, discrete processes [8]. This erroneous idea led to the creation of machines that were overly heavy and thick walled. It was believed that this provided high damping to the forces on the tool tips that were thought to be static. To properly predict chatter, one must realize that machining is a continuous, dynamic process with tooltip forces that are in constant fluctuation. When performing calculations, the specific characteristics of each machine must also be taken into consideration. If one takes two identical tools, placed into two identical machines, and perform the same machining process on two identical parts, the lifespan of the tools will not be the same. The dynamics and response of each of the machines differs slightly due to structural imperfections, imbalances, etc. Therefore, calculations must always take the machine-tool dynamics into consideration [23]. The modes of the machines structure determine the frequency and the direction that the tool is going to vibrate at [11]. Rather than the previously used machine design philosophy of "where there's vibration, add mass", it was then stated that designers must investigate the mode-forms, weak points, bearing clearances, and self-inducing vibratory components of their machine design to try to reduce chatter [8, 15]. Certain researchers even further investigatedthe required number of structural modes to produce accurate results [6]. Since it is impractical to investigate an unlimited bandwidth of a signal, restrictions must be made. This has generally been restrained to one or two modes of vibration of the machine. Their study proves that using low order models, that only incorporate two modes, are sufficiently accurate to model the machines.

In 1981, one of the first papers documenting the non-linearity of the vibratory system occurring during chatterwas published [20]. Self-excited chatter is a phenomenon that grows, but does not grow indefinitely. There is a point in time where the vibrations stabilize because of the tool jumping out of the cut. As the vibrations amplify, the tool head displacement increases. The displacement of the tool is not linear, but occurs in all three dimensions. When the force on the tool due to chatter causes displacement away from the work piece that exceeds the depth of cut, the tool will lose contact with the work piece. When this occurs, the work piece exerted forces on the tool all go to zero. The only forces acting on it now are the structural forces that want to keep the tool on its planned route. It is impossible for chatter to amplify further past this point, and so, this is where it stabilizes. Previous reports do not account for this stabilization. Their results are accurate up to this point, but then diverge from the experimentally obtained results. Tlusty's investigation was then complemented by

adding the behaviour of the tool after the onset of chatter [12]. The paper discusses the effects preceding passes of the tool have on the current state. It was generally accepted that wave patterns left on the work piece from a previous pass greatly effects the current pass, however, it is demonstrated that tool passes two or more turns prior to the current also have an effect. The phase difference and frequency of the waves etched into the surface of the prior turns interact with one another, and if the conditions are correct, interact in a critical way that produces increasing amplitude vibrations [10]. While Tlusty was able to theorize that chatter stabilizes at a certain point due to the tool leaving the work piece, [12] set off to prove this theory. They had the novel idea to turn the machine-work piece system into a circuit. Current was passed through the machine and into the work piece while turning. When chatter occurred, they noticed drops in current at the machine-tool contact point. This proves that an open circuit was being created, proving that the tool was losing contact with the work piece. They also sought out to prove why cutting becomes more stable at lower speeds. They believed that there was a resistive force caused by the tool moving forward along the cut. They found this resistive force to be inversely proportional to the cutting speed, and directly proportional to the relative velocity of the tool to the work piece. When this force was taken into account in their equations, it produces a wider region of stability while the spindle is at lower speeds. This resistive force was proven to be responsible for the large regions of stability at low spindle speeds, and is what diminishes at higher spindle speeds resulting in less stability. The majority of papers published prior to the 80's examined chatter with reference to the turning and boring processes. Milling is plagued with the same issues of chatter, but its modelling becomes more complicated. Tlusty and Ismail [21] characterized the chatter in the milling process by examining the periodicity of the forces that occur at the tool that are not present in other processes. During the milling process, cutter teeth come into and out of contact with the work piece. It is on the surface of these teeth that the force is applied. The same number of teeth are not always in contact with the work piece, and each tooth may be removing a different amount of material at a time. This leads to widely varying forces at the tool tip, creating a more challenging system to model. Forced vibrations can be attributed to periodic forces that the machine is subjected to. This can include an imbalance on rotating parts, or forces the machine transfers to the tool while moving. Chatter must be isolated from this in experiments so that the observations and calculations can be kept specific to the chatter phenomenon.

Once an accurate model of the milling process had been created, a reliable stability lobe can be constructed. Stability lobes plot the axial depth of cut vs. spindle speed. The resulting graph has a series of lobes that intersect each other at certain points. The area that is formed underneath the intersection of these lobes represents conditions that will produce stable machining. The area above these intersections represent unstable machining conditions. The concept of the stability lobe was first proposed by Tobias [24] As the mathematical modelling of the machining systems improved, so did the accuracy of the stability lobes. Prior to the paper by Tlusty *et al.* [22], most stability lobe calculations contained many simplifying assumptions, and therefore, were not very accurate; all teeth on the cutter were assumed to be oriented in the same direction, and also had a uniform pitch. They eliminated all of these assumptions and proved their math represented reality more accurately. A quarter of a cen-

turylater, Mann *et al.* [14] discovered unstable regions in a stability lobe graph that existed underneath the stability boundary for the milling operation. They resemble islands in the fact that they are ovular areas contained within the stable regions, complicating the previously thought simple stability lobe model. It was found that stability lobes taken from modal parameters of the machine at rest (static) were not as accurate as the stability lobes produced from the dynamic modal properties. Zaghbani & Songmene [25] obtained these dynamic properties using operational modal analysis (OMA). OMA uses the autoregressive moving average method and least square complex exponential method to obtain these values, producing a dynamic stability lobe that more accurately represents stable cutting conditions. These stability lobes have proven to be an invaluable asset to machinists and machine programmers. They provide a quick and easy reference to choose machining parameters that should produce a chatter free cut [2].

Tool wear is an often-overlooked factor that contributes to chatter. With the aid of more powerful computers this variable can now be included in simulations. The cutting tool is not indestructible and will change its shape while machining, and consequently affects the stability of the system and stability lobes [7]. As the tool becomes worn, its limits of stability increase. Therefore, the axial depth of cut can be increased while maintaining the same spindle speed that would have previously created chatter. The rate of wear was incorporated into the stability lobe calculations for the tools so that it was now also a function of wear. To verify their calculations, the tools were ground to certain stages of wear and then tested experimentally. They were found to be in strong agreement. Tool wear, however, is not something that machine shops want increased. Chatter increases the rates of tool wear, shortening their lifespan, and increasing the amount of money the shops must spend on new tools. Li *et al.* [13] determined that the coherence function of two crossed accelerations in the bending vibration of the tool shank approaches unity at the onset of chatter. A threshold needs to be set [16] and then detected using simple mechanism to alert the operator to change the machining conditions and avoid increased tool wear.

In most of the previous stability prediction methods, a Frequency Response Function (FRF) is required to perform the calculations. FRF refers to how the machine's structure reacts to vibration. It is required to do an impact test to acquire the system's FRF [17]. In this case, an accelerometer is placed at the end of the top of the tool, and a hammer is used to strike the tool. The accelerometer will measure the displacement of the tool, telling the engineer how the machine reacts to vibration. This test gives crucial information about the machine, such as the damping of the structure and its natural frequencies. This method of obtaining information is impractical; because the FRF of the machine is always changing, it would require the impact test to be performed at all the different stages of machining. Also, having to do this interrupts the manufacturing processing and having machines sitting idle costs the company money. An offline method of obtaining this information could greatly benefit machining companies by eliminating the need for the impact test. Adetoro *et al.* [1] proposed that the machine, tool and work piece could be modelled using finite element analysis.A computer simulation would be able to predict the FRF during all phases of the machining process. As the part is machined and becomes thinner, its response to vibration changes

dramatically. Previous research papers assume a constant FRF throughout the whole proc‐ ess for the sake of reducing computations. However, a constantly updated FRF would allow for accurate, real time stability calculations.

To the authors' best knowledge, the spindle decay/bearings wear over the service time and their effects on the system natural frequencies, and consequently change of the stability lobes, have not been investigated.The objective of the present study is to determine the natu‐ ral frequencies/vibration characteristics ofmachine tool spindle systems by developing its Dynamic Stiffness Matrix (DSM) [4] and applying the proper boundary conditions. These re‐ sults would then be compared to the experimental results obtained from testing a common cutting system to validate/tune the model developed. The Hamilton's Principle is used to derive the differential equations governing the coupled Bending-Bending (B-B) vibration of a spinning beam, which are solved for harmonic oscillations. A MATLAB® code is devel‐ oped to assemble the DSM element matrices for multiple components and applying the boundary conditions (BC). The machine spindles usually contain bearings, simulated by ap‐ plying spring elements at said locations. The bearings are first modeled as Simply-Support‐ ed (S-S) frictionless pins. The S-Sboundary conditions are then replaced by linear spring elements to incorporate the flexibility of bearings into the DSM model. In comparison with the manufactures' data on the spindle's fundamental frequency, the bearing stiffness coeffi‐ cients, K_S, are then varied to achieve a Calibrated Dynamics Stiffness Matrix (CDSM) vibra‐ tional model. Once the non-spinning results are confirmed and the spindle model tuned to represent the real system, the formulation could then be extended to include varying rota‐ tional speeds and torsional degree-of-freedom (DOF) for further modeling purposes. The re‐ search outcomepresented in this Chapter is to be used in the next phase of the authors' ongoing research to establish the relationship between the tool/system characteristics (incor‐ porating spindle's service time/age), and intended machining process, through the develop‐ ment of relevant Stability Lobes, to achieve the best results.

2. Mathematical model

Computer Numeric Control (CNC) machines are quite often found in industries where a great deal of machining occurs. These machines are generally 3-, 4- or 5-axis, depending on the number of degrees of freedom the device has. Having the tool translate in the X, Y and Z direction accounts for the first three degrees-of-freedom (DOF). Rotation about the spindle axes account for any further DOF. The spindle contains the motors that rotate the tools and all the mechanisms that hold the tool in place. Figure 1 displays a sample spindle configura‐ tion and a typical tool/holder configuration is shown in Figure 2.
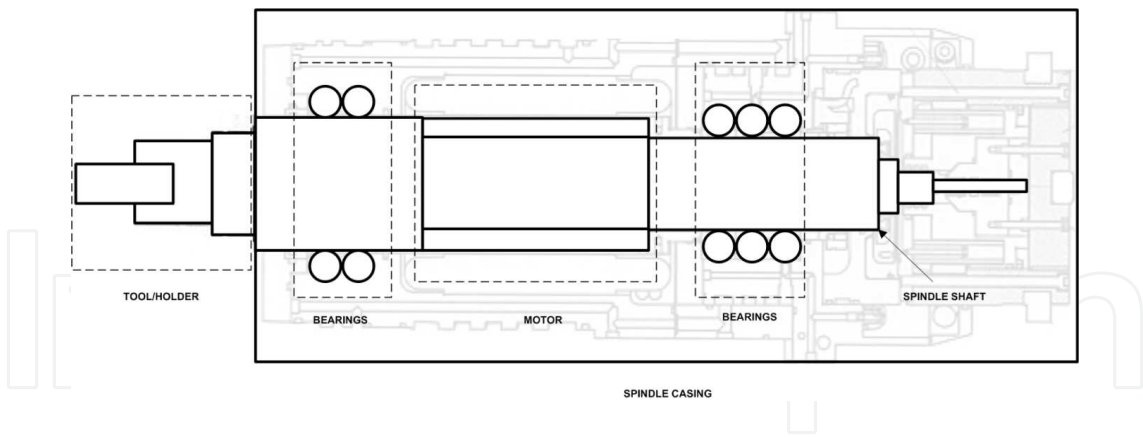
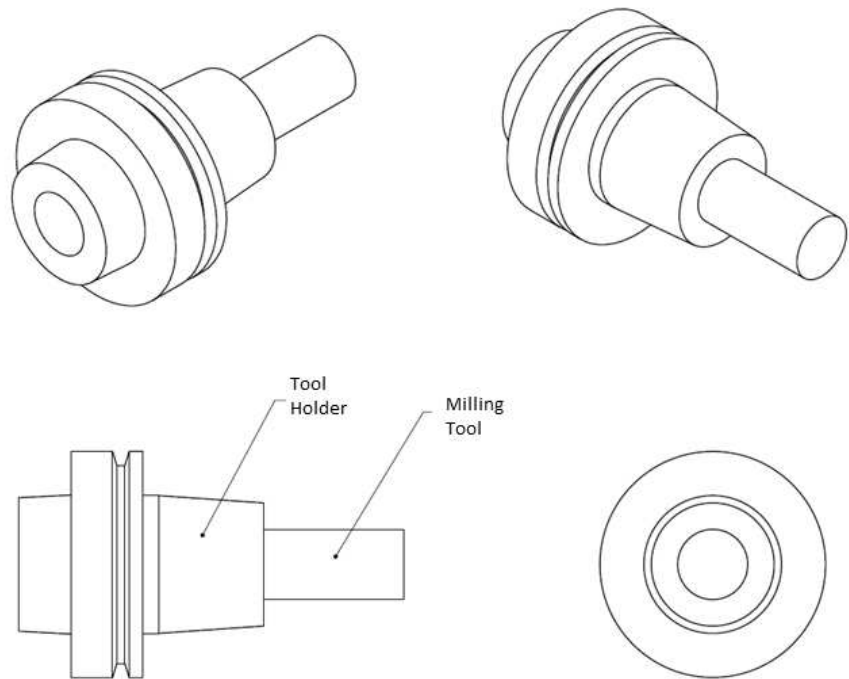**Figure 1.** Typical Spindle Configuration.

Figure 2. Typical Tool/Holder Configuration.

In this section, following the assumptions made by Banerjee & Su [5], discarding torsional vibrations, neglecting the rotary ineriaand shear deformation effects, the development of the governing differential equations of motion for coupled Bending-Bending (B-B) vibratins of a spinning beam is first briefly discussed. Then, based on the general procedure presented by Banerjee [4], the development of Dynamic Stiffness Matrix (DSM) formulation of the problem is conciselypresented. Figure 3 shows the spinnning beam, represented by a cylinder in a right-handed rectangular Cartesian coordinates system. The beam length is L, mass per unit length is $m=\rho A$, and the bending rigidities are EI_{xx} and EI_{yy}. See Figure 4 for the Degrees-of-Freedom (DOF) of the system.
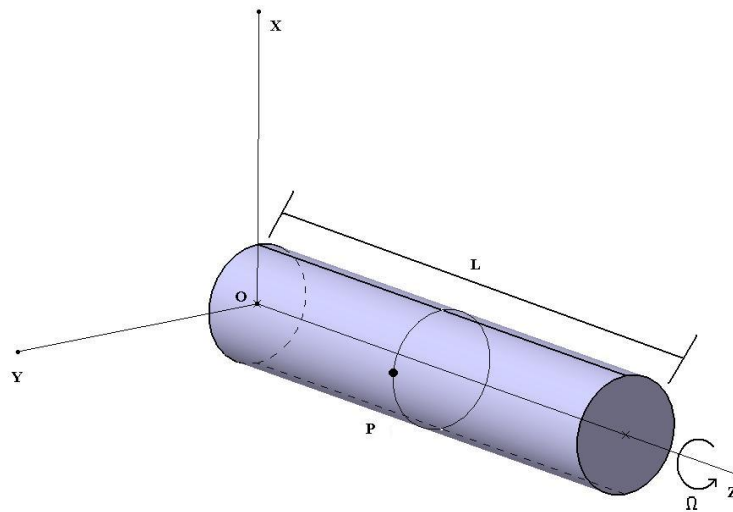
Figure 3. Spinning Beam.
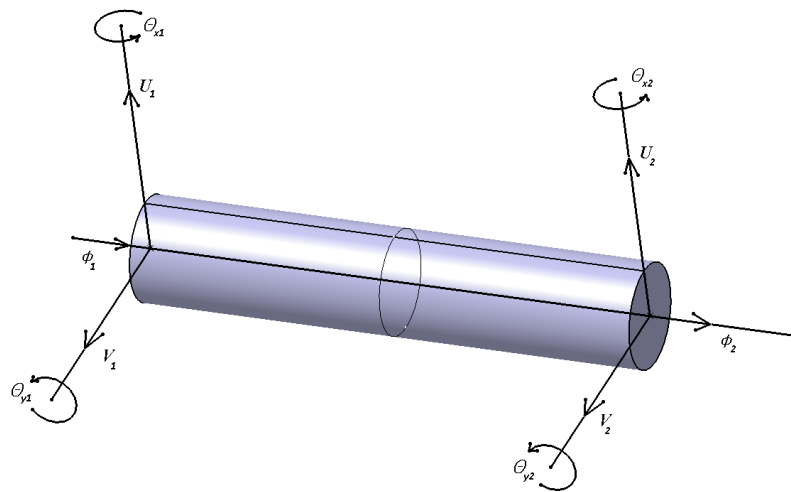
Figure 4. Degrees-of-Freedom (DOF) of the system

At an arbitrary cross section, located at z from O, u and v are lateral displacements of a point P in the X and Y directions, respectively. The cross section is allowed to rotate or twist about the OZ axis. The position vector $\boldsymbol{r}$ of the point P after deformation is given by

$$\boldsymbol{r} = \left(\text{u} - \phi \text{y} \right) \boldsymbol{i} + \left(\text{v} + \phi \text{x} \right) \boldsymbol{j} \tag{1}$$

where $\boldsymbol{i}$ and $\boldsymbol{j}$ are unit vectors in the X and Y directions, respectively. The velocity of point P is given by

$$\mathbf{v} = \dot{\mathbf{r}} + \boldsymbol{\Omega} \times \mathbf{r}, \ \textit{where} \ \boldsymbol{\Omega} = \Omega \mathbf{k} \tag{2}$$

The kinetic and potential energies of the beam (T and U) are given by:

$$T = \frac{1}{2}\int_0^L |v|^2 \, mdz = \frac{1}{2}m\int_0^L [\dot{u}^2 + \dot{v}^2 + 2\Omega(u\dot{v} - \dot{u}v) + \Omega^2(u^2 + v^2)]dz, \tag{3}$$

$$U = \frac{1}{2}EI_{xx}\int_0^L v''^2 dz + \frac{1}{2}EI_{yy}\int_0^L u''^2 dz \tag{4}$$

Using the Hamilton Principle in the usual notation state

$$\delta\int_{t_1}^{t_2}(T - U)dt = 0, \tag{5}$$

where t_1 and t_2 are the time intervals in the dynamic trajectory and δ is the variational operator. Substituting the kinetic and potential energies in the Hamilton Principle, collecting like terms and integrating by parts, leads to the following set of equations.

$$EI_{yy}u'''' - m\Omega^2 u + m\ddot{u} - 2m\Omega\dot{v} = 0, \tag{6}$$

$$-2m\Omega\dot{u} - EI_{xx}v'''' - m\ddot{v} + m\Omega^2 v = 0. \tag{7}$$

The resulting loads are then found to be in the following forms, written for Shear forces as

$$S_x = EI_{xx}u''', \ \text{and} \ S_y = EI_{yy}v''', \tag{8}$$

and for Bending Moments as

$$M_x = EI_{xx}v'', \ \text{and} \ M_y = -EI_{yy}u''. \tag{9}$$

Assuming the simple harmonic motion, the form of

$$u(z,\ t) = U(z)\sin\omega t, \ \text{and} \ v(z,\ t) = V(z)\cos\omega t \tag{10}$$

where ω frequency of oscillation and U and V are the amplitudes of u and v . Substituting equations (10) into equations (6) and (7), they can be re-written as:

$$\left(EI_{yy}U'''' - m(\Omega^2 + \omega^2)U\right) + 2m\Omega\omega V = 0, \tag{11}$$

$$\left(EI_{xx}V'''' - m(\Omega^2 + \omega^2)V\right) + 2m\Omega\omega U = 0. \tag{12}$$

Introducing $\xi = z/L$ and $D = d/d\xi$, which are non-dimensional length and the differential operator into equations (11) and (12) leads to

$$\left[D^4 - \frac{m(\omega^2 + \Omega^2)L^4}{EI_{yy}}\right]U + \frac{2m\Omega\omega L^4}{EI_{yy}}V = 0, \tag{13}$$

$$\left[D^4 - \frac{m(\omega^2 + \Omega^2)L^4}{EI_{xx}}\right]V + \frac{2m\Omega\omega L^4}{EI_{xx}}U = 0. \tag{14}$$

The above equations are combined to form the following 8th-order differential equation,

$$\left[D^8 - \left(\lambda_x^2 + \lambda_y^2\right)(1 + \eta^2)D^4 + \lambda_x^2\lambda_y^2(1 - \eta^2)^2\right]W = 0 \tag{15}$$

written in terms of W, satisfied by both U and V, where

$$\lambda_x^2 = \frac{m\omega^2 L^4}{EI_{xx}}, \quad \lambda_y^2 = \frac{m\omega^2 L^4}{EI_{yy}}, \quad \text{and} \quad \eta^2 = \frac{\Omega^2}{\omega^2} \tag{16}$$

The solution of the differential equation is sought in the form $W = e^{r\xi}$, and when substituted into (15), leads to

$$r^8 - \left(\lambda_x^2 + \lambda_y^2\right)(1 + \eta^2)r^4 + \lambda_x^2\lambda_y^2(1 - \eta^2)^2 \tag{17}$$

where

$$r_{1,3} = \pm\sqrt{\alpha}, \quad r_{2,4} = \pm\sqrt{\beta}, \quad r_{5,7} = \pm i\sqrt{\alpha}, \quad r_{6,8} = \pm i\sqrt{\beta},$$

and

$$\alpha^2 = \frac{1}{2}\left\{\left(\lambda_x^2 + \lambda_y^2\right)(1 + \eta^2) + \sqrt{\left(\lambda_x^2 - \lambda_y^2\right)^2(1 + \eta^2)^2 + 16\lambda_x^2\lambda_y^2\eta^2}\right\},$$

$$\beta^2 = \frac{1}{2}\left\{\left(\lambda_x^2 + \lambda_y^2\right)(1 + \eta^2) - \sqrt{\left(\lambda_x^2 - \lambda_y^2\right)^2(1 + \eta^2)^2 + 16\lambda_x^2\lambda_y^2\eta^2}\right\} \tag{18}$$

From the above solutions of U and V, the corresponding bending rotation about X and Y axes, Θ_x and Θ_y, respectively, are given by

$$\Theta_x = \frac{dV}{dz} = -\frac{1}{L}\frac{dV}{d\xi} =$$

$$-\frac{1}{L}\begin{pmatrix} \sqrt{\alpha}B_1\cos\sqrt{\alpha}\xi - \sqrt{\alpha}B_2\sin\sqrt{\alpha}\xi + \\ \sqrt{\alpha}B_3\cosh\sqrt{\alpha}\xi + \sqrt{\alpha}B_4\sinh\sqrt{\alpha}\xi + \sqrt{\beta}B_5\cos\sqrt{\beta}\xi - \\ \sqrt{\beta}B_6\sin\sqrt{\beta}\xi + \sqrt{\beta}B_7\cosh\sqrt{\beta}\xi + \\ \sqrt{\beta}B_8\sinh\sqrt{\beta}\xi \end{pmatrix},$$

$$\Theta_y = \frac{dU}{dz} = \frac{1}{L}\frac{dU}{d\xi} =$$

$$-\frac{1}{L}\begin{pmatrix} \sqrt{\alpha}A_1\cos\sqrt{\alpha}\xi - \sqrt{\alpha}A_2\sin\sqrt{\alpha}\xi + \\ \sqrt{\alpha}A_3\cosh\sqrt{\alpha}\xi + \sqrt{\alpha}A_4\sinh\sqrt{\alpha}\xi + \sqrt{\beta}A_5\cos\sqrt{\beta}\xi - \\ \sqrt{\beta}A_6\sin\sqrt{\beta}\xi + \sqrt{\beta}A_7\cosh\sqrt{\beta}\xi + \sqrt{\beta}A_8\sinh\sqrt{\beta}\xi \end{pmatrix}.$$

$$(19)$$

By doing similar substitutions we find

$$S_x = \left(\frac{EI_{yy}}{L^3}\right)\begin{pmatrix} -\alpha\sqrt{\alpha}A_1\cos\sqrt{\alpha}\xi + \alpha\sqrt{\alpha}A_2\sin\sqrt{\alpha}\xi + \\ \alpha\sqrt{\alpha}A_3\cosh\sqrt{\alpha}\xi + \alpha\sqrt{\alpha}A_4\sinh\sqrt{\alpha}\xi - \\ \beta\sqrt{\beta}A_5\cos\sqrt{\beta}\xi + \beta\sqrt{\beta}A_6\sin\sqrt{\beta}\xi + \beta\sqrt{\beta}A_7\cosh\sqrt{\beta}\xi \\ +\beta\sqrt{\beta}A_8\sinh\sqrt{\beta}\xi \end{pmatrix}$$

$$S_y = \left(\frac{EI_{xx}}{L^3}\right)\begin{pmatrix} -\alpha\sqrt{\alpha}B_1\cos\sqrt{\alpha}\xi + \alpha\sqrt{\alpha}B_2\sin \\ \sqrt{\alpha}\xi + \alpha\sqrt{\alpha}B_3\cosh\sqrt{\alpha}\xi + \alpha\sqrt{\alpha}B_4\sinh\sqrt{\alpha}\xi - \\ \beta\sqrt{\beta}B_5\cos\sqrt{\beta}\xi + \beta\sqrt{\beta}B_6\sin\sqrt{\beta}\xi + \\ \beta\sqrt{\beta}B_7\cosh\sqrt{\beta}\xi + \beta\sqrt{\beta}B_8\sinh\sqrt{\beta}\xi \end{pmatrix}$$

$$(20)$$

$$M_x = \left(\frac{EI_{yy}}{L^2}\right)\begin{pmatrix} -\alpha B_1\sin\sqrt{\alpha}\xi - \alpha B_2\cos\sqrt{\alpha}\xi + \\ \alpha B_3\sinh\sqrt{\alpha}\xi + \alpha B_4\cosh\sqrt{\alpha}\xi - \beta B_5\sin\sqrt{\beta}\xi + \\ \beta B_6\cos\sqrt{\beta}\xi + \beta B_7\sinh\sqrt{\beta}\xi + \beta B_8\cosh\sqrt{\beta}\xi \end{pmatrix}$$

$$M_y = \left(\frac{EI_{xx}}{L^2}\right)\begin{pmatrix} -\alpha A_1\sin\sqrt{\alpha}\xi - \alpha A_2\cos\sqrt{\alpha}\xi + \\ \alpha A_3\sinh\sqrt{\alpha}\xi + \alpha A_4\cosh\sqrt{\alpha}\xi - \\ \beta A_5\sin\sqrt{\beta}\xi + \beta A_6\cos\sqrt{\beta}\xi + \beta A_7\sinh\sqrt{\beta}\xi, \\ +\beta A_8\cosh\sqrt{\beta}\xi \end{pmatrix},$$

where

$$A_1 = k_\alpha B_1, \ A_2 = k_\alpha B_2, \ A_3 = k_\alpha B_3, \ A_4 = k_\alpha B_4,$$
$$A_5 = k_\beta B_5, \ A_6 = k_\beta B_6, \ A_7 = k_\beta B_7, \ A_8 = k_\beta B_8$$

with

$$k_\alpha = \frac{2\lambda_y^2 \eta}{\alpha^2 - \lambda_y^2(1 + \eta^2)}, \text{ and } k_\beta = \frac{2\lambda_y^2 \eta}{\beta^2 - \lambda_y^2(1 + \eta^2)}. \tag{21}$$

To obtain the dynamic stiffness matrix (DSM) of the system the boundary conditions are then introduced into the governing equations.

For Displacements:

$$At \, z = 0: \quad U = U_1, \ V = V_1, \ \Theta_x = \Theta_{x1}, \ \Theta_y = \Theta_{y1}$$
$$At \, z = L: \quad U = U_2, \ V = V_2, \ \Theta_x = \Theta_{x2}, \ \Theta_y = \Theta_{y2} \tag{22}$$

For Forces we have

$$At \, z = 0: \quad S_x = S_{x1}, \ S_y = S_{y1} \ , M_x = M_{x1} = M_y = M_{y1,}$$
$$At \, z = L: \quad S_x = S_{x2}, \ S_y = S_{y2} \ , M_x = M_{x2} = M_y = M_{y2.} \tag{23}$$

Substituting the boundary conditions into the governing equations we find

$$\boxed{\delta = \mathbf{B} \, \mathbf{R}} \tag{24}$$

where

$$\delta = [U_1 V_1 \Theta_{x1} \Theta_{y1} U_2 V_2 \Theta_{x2} \Theta_{y2}]^T,$$
$$\mathbf{R} = [R_1 R_2 R_3 R_4 R_5 R_6 R_7 R_8]^T, \tag{25}$$

and

$$
\mathbf{B} = \begin{bmatrix}
0 & k_\alpha & 0 & k_\alpha & 0 & k_\beta & 0 & k_\beta \\
0 & 1 & 0 & 1 & 0 & 1 & 0 & 1 \\
-\tau_\alpha & 0 & -\tau_\alpha & 0 & -\tau_\beta & 0 & -\tau_\beta & 0 \\
\chi_\alpha & 0 & \chi_\alpha & 0 & \chi_\beta & 0 & \chi_\beta & 0 \\
k_\alpha S_\alpha & k_\alpha C_\alpha & k_\alpha S_{h_\alpha} & k_\alpha C_{h_\alpha} & k_\beta S_\beta & k_\beta C_\beta & k_\beta S_{h_\beta} & k_\beta C_{h_\beta} \\
S_\alpha & C_\alpha & S_{h_\alpha} & C_{h_\alpha} & S_\beta & C_\beta & S_{h_\beta} & C_{h_\beta} \\
-\tau_\alpha C_\alpha & \tau_\alpha S_\alpha & -\tau_\alpha C_{h_\alpha} & -\tau_\alpha S_{h_\alpha} & -\tau_\beta C_\beta & \tau_\beta S_\beta & -\tau_\beta C_{h_\beta} & -\tau_\beta S_{h_\beta} \\
\chi_\alpha C_\alpha & -\chi_\alpha S_\alpha & \chi_\alpha C_{h_\alpha} & \chi_\alpha S_{h_\alpha} & \chi_\beta C_\beta & -\chi_\beta S_\beta & \chi_\beta C_{h_\beta} & \chi_\beta S_{h_\beta}
\end{bmatrix}
\tag{26}
$$

with,

$$
\tau_\alpha = \frac{\sqrt{\alpha}}{L}, \ \tau_\beta = -\frac{\sqrt{\beta}}{L}, \ \omega_\alpha = k_\alpha \tau_\alpha, \ \omega_\beta = k_\beta \tau_\beta,
$$

$$
\begin{aligned}
S_\alpha &= \sin\sqrt{\alpha}, & C_\alpha &= \cos\sqrt{\alpha}, & S_{h_\alpha} &= \sinh\sqrt{\alpha}, & C_{h_\alpha} &= \cosh\sqrt{\alpha}, \\
S_\beta &= \sin\sqrt{\beta}, & C_\beta &= \cos\sqrt{\beta}, & S_{h_\beta} &= \sinh\sqrt{\beta}, & C_{h_\beta} &= \cosh\sqrt{\beta}.
\end{aligned}
\tag{27}
$$

Substituting similarly for the force equation

$$
\boxed{\mathbf{F} = \mathbf{A}\,\mathbf{R}}
\tag{28}
$$

where

$$
\mathbf{F} = [S_{x1} S_{y1} M_{x1} M_{y1} S_{x2} S_{y2} M_{x2} M_{y2}]^T,
\tag{29}
$$

$$
\mathbf{A} = \begin{bmatrix}
-\zeta_\alpha & 0 & \zeta_\alpha & 0 & -\zeta_\beta & 0 & \zeta_\beta & 0 \\
-\varepsilon_\alpha & 0 & \varepsilon_\alpha & 0 & -\varepsilon_\beta & 0 & \varepsilon_\beta & 0 \\
0 & -\gamma_\alpha & 0 & \gamma_\alpha & 0 & -\gamma_\beta & 0 & \gamma_\beta \\
0 & \lambda_\alpha & 0 & -\lambda_\alpha & 0 & \lambda_\beta & 0 & -\lambda_\beta \\
\zeta_\alpha C_\alpha & -\zeta_\alpha S_\alpha & -\zeta_\alpha C_{h_\alpha} & -\zeta_\alpha S_{h_\alpha} & \zeta_\beta C_\beta & -\zeta_\beta S_\beta & -\zeta_\beta C_{h_\beta} & -\zeta_\beta S_{h_\beta} \\
\varepsilon_\alpha C_\alpha & -\varepsilon_\alpha S_\alpha & -\varepsilon_\alpha C_{h_\alpha} & -\varepsilon_\alpha S_{h_\alpha} & \varepsilon_\beta C_\beta & -\varepsilon_\beta S_\beta & -\varepsilon_\beta C_{h_\beta} & -\varepsilon_\beta S_{h_\beta} \\
\gamma_\alpha S_\alpha & \gamma_\alpha C_\alpha & -\gamma_\alpha S_{h_\alpha} & -\gamma_\alpha C_{h_\alpha} & \gamma_\beta S_\beta & \gamma_\beta C_\beta & -\gamma_\beta S_{h_\beta} & -\gamma_\beta C_{h_\beta} \\
-\lambda_\alpha S_\alpha & -\lambda_\alpha C_\alpha & \lambda_\alpha S_{h_\alpha} & \lambda_\alpha C_{h_\alpha} & -\lambda_\beta S_\beta & -\lambda_\beta C_\beta & \lambda_\beta S_{h_\beta} & \lambda_\beta C_{h_\beta}
\end{bmatrix}
\tag{30}
$$

and

$$\zeta_\alpha = k_\alpha \alpha \sqrt{\alpha} \frac{EI_{yy}}{L^3}, \ \eta_\alpha = \alpha \sqrt{\alpha} \frac{EI_{xx}}{L^3}, \ \gamma_\alpha = \alpha \frac{EI_{xx}}{L^2}, \ \lambda_\alpha = k_\alpha \alpha \frac{EI_{yy}}{L^2},$$

$$\zeta_\beta = k_\beta \beta \sqrt{\beta} \frac{EI_{yy}}{L^3}, \ \eta_\beta = \beta \sqrt{\beta} \frac{EI_{xx}}{L^3}, \ \gamma_\beta = \beta \frac{EI_{xx}}{L^2}, \ \lambda_\beta = k_\beta \beta \frac{EI_{yy}}{L^2}.$$

(31)

The frequency-dependent dynamic stiffness matrix (DSM) of the spinning beam, $\mathbf{K(\omega)}$,can be derived by eliminating $\mathbf{R}$. The force amplitude is related to the displacement vector by

$$\mathbf{F = K\delta}$$

(32)

For that we find

$$\mathbf{F = K(B \ R) = A \ R}$$

(33)

and assuming *KB = A*, finally leads to

$$\mathbf{K(\omega) = AB^{-1}}$$

(34)

Once the correctness and accuracy of the DSM code was established, a real machine spindle was then modeled, where the non-uniform spindle was idealized as a piecewise uniform (stepped) beam. Each step was modeled as a single continuous element and the above steps in the DSM formulation are repeated several times to determine the stiffness matrix for each element of the spindle. The element Dynamic Stiffness matrices are then assembled and the boundary conditions are applied. The system is simplified to contain 12 elements (13 nodes), as shown in Figure 5.
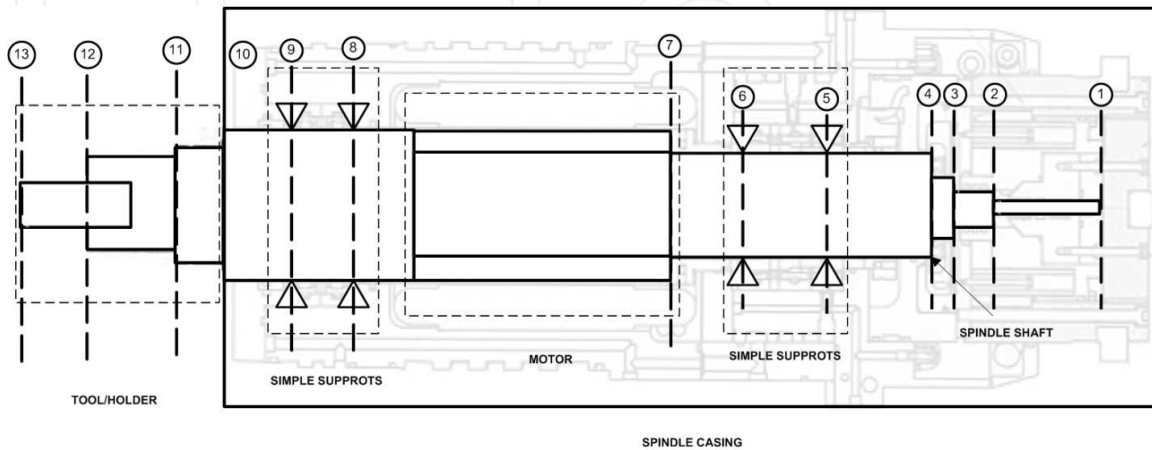
Figure 5. Simplified Spindle sections, with bearings modeled as simply-supported BC.

It is assumed that the entire system is made from the same material and the properties of tooling steel were used for all section. It was also assumed that the system is simply supported at the locations of the bearings. The simply supported boundary conditions were then modified and replaced by linear spring elements (Figure 6); the spring stiffness values were varied in an attempt to achieve a fundamental frequency equivalent to the spindle system's natural frequency reported by the manufacturer.
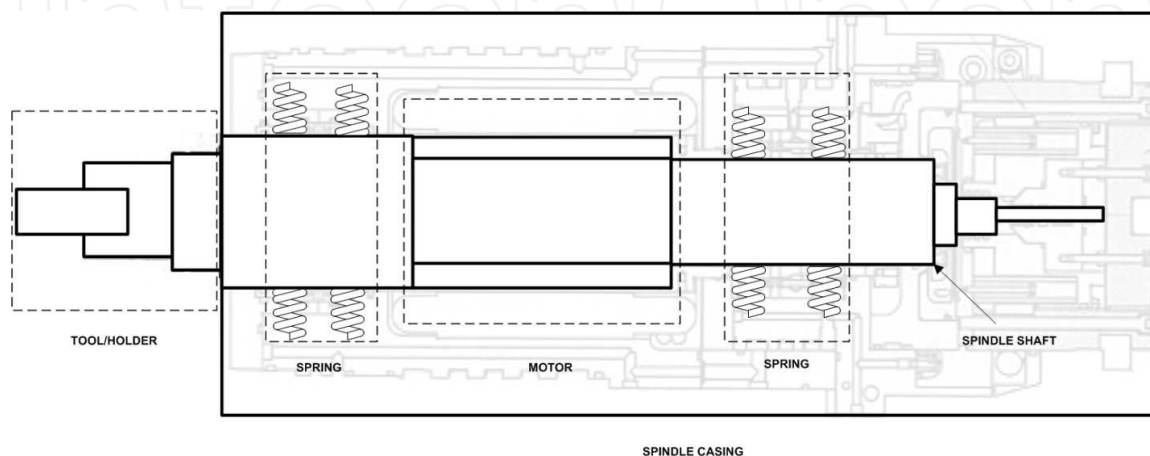
Figure 6. Spindle model, with bearings modeled as linear spring elements(modified BC).

## 3. Numerical tests and experimental results

3.1. DSM results

When the spindle was modeled using simply supported boundary conditions at the bearing locations, the fundamental natural frequency of the system was found to be just below 1400 Hz, i.e., higher than the nominal value provided by the manufacturer. The boundary conditions were then updated and the simple supports (bearings) were replaced by spring elements. The new spring-supported model was then updated/calibrated to achieve the spindle's nominal fundamental natural frequency by varying spring stiffness values, K_s, all assumed to be identical. It was observed that as the spring stiffness value increase the natural frequency of the system increases. The natural frequency then levels out and reaches an asymptote as the springs start behaving more like simple supports at high values of spring stiffness. It was also found that at spring stiffness value of $K_s = 2.1 \times 10^8$ N/m the system achieves the natural frequency reported by the spindle manufacturer. This value of spring stiffness will be used for any further analysis of the system. These results are shown in Figure 7.

Using the above results the natural frequency of the spindle was also found for multiple rotational speeds (Figure 8). It was observed that, as expected, as the spindle rotation speed increases the natural frequency of the system decreases. It was also found that the spindle

critical spindle speed is 2.3×10^6 RPM which is well above the operating rotational speed of the spindle, i.e., 3.5×10^4 RPM.
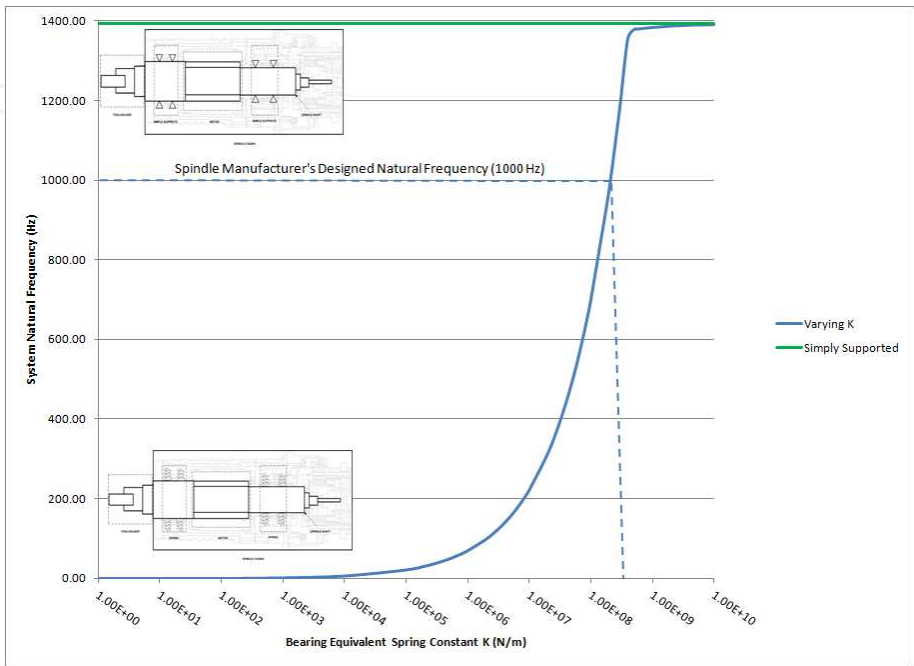

Figure 7. System Natural Frequency vs. Bearing Equivalent Spring Constant (in log scale).
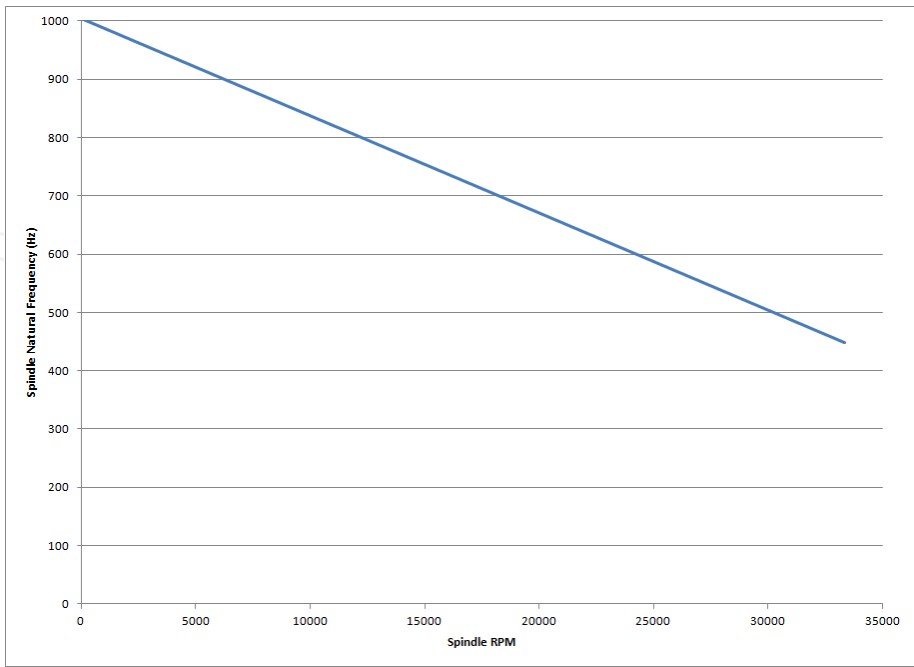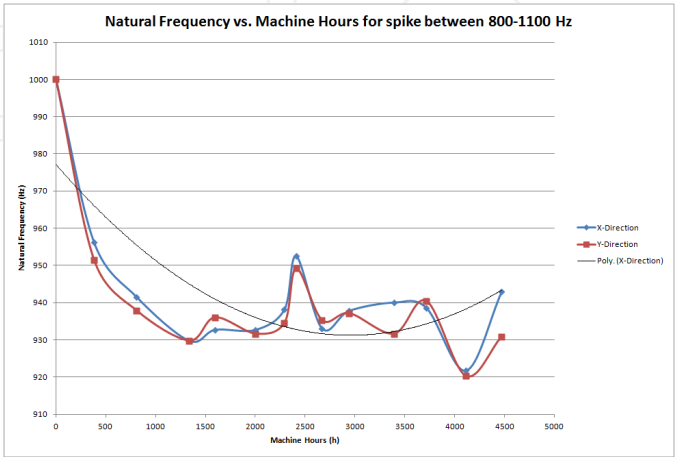

Figure 8. Spindle Natural Frequency vs. Spindle RPM.

3.2. Preliminary Experimental results

The experimentally evaluated Frequency Response Function (FRF) data were collected for a machine over the period of twelve months. A 1-inch diameter blank tool with a 2-inch protrusion was used. A typical shrink fit tool holder was also used (See Figure 9). This type of holder was selected for its rigid contact surface with the tool. Therefore, any play in the whole system was going to be attributed to the spindle. The tested machine was used to produce typical machined parts and was not restricted to one type of cut. This was done to observe the spindle decay over time while operating under normal production conditions. The tool was placed in the spindle and the spindle was returned to its neutral position as shown in Figure 9. Acceleration transducers were placed in both the X and Y direction. The tool was struck with an impulse hammer in both the X and Y directions and corresponding bending natural frequencies were evaluated over the time. Figure 10 shows the bending natural frequencies of the non-spinning spindle vs. machine hours. As can be seen, system natural frequencies in both X and Y directions reduce with spindle's life, which can be attributed to bearings decay. Further reseatrch is underway to analyze more spindles and to model the system decay by establishing a relationship between bearings stiffness, K_s, and machine hours. This, in turn, can be used to predict the optimum machining parameters as a function of spindle age.
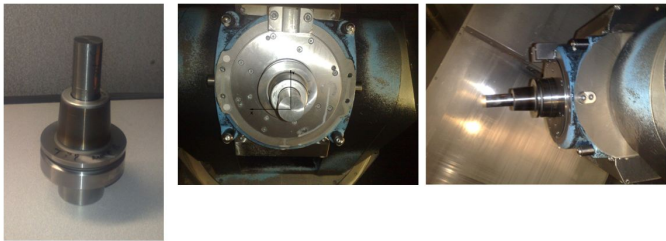
Figure 9. Blank Tool (left) and Blank Tool in Spindle (middle and right).

Figure 10. Natural Frequency vs. Machine Hours.

4. Conclusion

The effects of spindle system's vibrational behavior on the stability lobes, and as a result on the Chatter behavior of machine tools have been established. It has been observed that the service life changes the vibrational behavior of spindles, i.e., reduced natural frequency over the time. An analytical model of a multi-segment spinning spindle, based on the Dynamic Stiffness Matrix (DSM) formulation and exact within the limits of the Euler-Bernoulli beam bending theory, was developed. The beam exhibits coupled Bending-Bending (B-B) vibration and, as expected, its natural frequencies are found to decrease with increasing spinning speed. The bearings were included in the model using two different models; rigid, simply-supported, frictionless pins and flexible linear spring elements. The linear spring element stiffness, K_s, was then calibrated so that the fundamental frequency of the system matched the nominal data provided by the manufacturer. This step is vital to the next phase of the authors' ongoing research, where the bearing wear would be modeled in terms of spindle's service time/age, to investigate the consequent effects on the stability lobes and, in turn, on themachine Chatter.

Acknowledgements

Author details

Seyed M. Hashemi[*] and Omar Gaber

*Address all correspondence to: smhashem@ryerson.ca

Department of Aerospace Eng., Ryerson University, Toronto (ON), Canada

References

[1] Adetoro, O. B. , Wen, P. H., Sim, W. M., & Vepa, R. (2009, 1-3 July). Stability Lobes Prediction in Thin Wall Machining. Paper presented at World Congress on Engineering, WCE 2009, London, U.K. 520-525, 978-9-88170-125-1.

[2] Altintas, Y., & Budak, E. (1995). Analytical Prediction of Stability Lobes in Milling. *CIRP Annals- Manufacturing Technology*, 44(1), 357-362, 0007-8506.

[3] Arnold, R. N. (1946). Discussion on the Mechanism of Tool Vibration in the Cutting of Steel. *Proceedings of the Institution of Mechanical Engineers*, 154, 429-432.

[4] Banerjee, J. R. (1997, April). Dynamic Stiffness Formulation for Structural Elements: A General Approach. *Computers & Structures*, 63(1), 101-103, 0045-7949.

[5] Banerjee, J. R., & Su, H. (2004, September-October). Development of a Dynamic Stiffness Matrix for Free Vibration Analysis of Spinning Beams. *Computers and Structures*, 82(23-26), 2189-2197, 0045-7949.

[6] Butlin, T., & Woodhouse, J. (2009, November). Friction-Induced Vibration: Should Low-Order Models be Believed. *Journal of Sound and Vibration*, 328(1-2), 92-108, 0002-2460X.

[7] Clancy, B. E., & Shin, Y. C. (2002, July). A Comprehensive Chatter Prediction Model for Face Turning Operation Including Tool Wear Effect. *International Journal of Machine Tools and Manufacture*, 42(9), 1035-1044, 0890-6955.

[8] Eisele, F. (1961, December). Machine Tool Research at the Technological University of Munich. *International Journal of Machine Tool Design Research*, 1(4), 249-274, 0890-6955.

[9] Gurney, J. P., & Tobias, S. A. (1961, September). A Grphical Method for the Determination of the Dynamic Stability of Machine Tools. *International Journal of Machine Tool Design Research*, 1(1-2), 148-156, 0020-7357.

[10] Heisel, U. (1994). Vibrations and Surface Generation in Slab Milling. *CIRP Annals-Manufacturing Technology*, 43(1), 337-340, 0007-8506.

[11] Insperger, T., Mann, B. P., Stepan, G., & Bayly, P. V. (2003, April). Multiple Chatter Frequencies in Milling Processes. *Journal of Sound and Vibration*, 262(2), 333-345, 0002-2460X.

[12] Yoshitaka, K., Osame, K., & Hisayoshi, S. (1981, November). Behaviour of Self Excited Chatter Due to Multiple Regenerative Effect. *Journal of Engineering for Industry*, 103(4), 324-329, 0022-1817.

[13] Li, X. Q., Wong, Y. S., & Nee, A. Y. C. (1997, April). Tool Wear and Chatter Detection using the Coherence Function of Two Crossed Accelerations. *International Journal of Machine Tools and Manufacture*, 37(4), 425-435, 0890-6955.

[14] Mann, B. P., Edes, B. T., Easly, S. J., Young, K. A., & Ma, K. (2008, March). Chatter Vibration and Surface Location Error Prediction for Helical End Mills. *International Journal of Machine Tools and Manufacture*, 48(3-4), 350-361, 0890-6955.

[15] Peng, Z. K., Jackson, M. R., Guo, L. Z., Parkin, R. M., & Meng, G. (2010, October). Effects of Bearing Clearance on the Chatter Stability of Milling Process. *Nonlinear Analysis: Real World Applications*, 11(5), 3577-3589, 1468-1218.

[16] Rahman, M., & Ito, Y. (1986, September). Detection of the Onset of Chatter Vibration. *Journal of Sound and Vibration*, 109(2), 193-205, 0002-2460X.

[17] Solis, E., Peres, C. R., Jimenez, J. E., Alique, J. R., & Monje, J. C. (2004). A New Analytical-Experimental Method for the Identification of Stability Lobes in High-Speed

Milling. International Journal of Machine Tools and Manufacture December) 0890-6955 , 44(15), 1591-1597.

[18] Taylor, F. W. (1907). On the Art of Cutting Metal. *Trans. ASME*, 28, 31-350.

[19] Shabana, A., & Thomas, B. (1987). Chatter Vibration of Flexible Multibody Machine Tool Mechanisms. *Mechanical Machine Theory*, 22(4), 359-369, 0009-4114X.

[20] Tlusty, J., & Ismail, F. (1981). Basic Non-Linearity in Machining Chatter. *CIRP Annals-Manufacturing Technology*, 30(1), 299-304, 0007-8506.

[21] Tlusty, J., & Ismail, F. (1983, January). Special Aspects if Chatter in Milling. *Journal of Vibration, Acoustics, Stress, and Reliability in Design*, 105(1), 24-32, 0739-3717.

[22] Tlusty, J., Zaton, W., & Ismail, F. (1983). Stability Lobes in Milling. CIRP Annals-Manufacturing Technology 0007-8506 , 32(1), 309-313.

[23] Tobias, S. A., & Andrew, C. (1962, October-December). Vibration in Horizontal Milling. *International Journal of Machine Tool Design Research*, 2(4), 369-378, 0890-6955.

[24] Tobias, S. A. (1965). Machine Tool Vibration. Blackie and Sons Ltd. London, Glasgow

[25] Zaghbani, I., & Songmene, V. (2009, October). Estimation of Machine-Tool Dynamic Parameters During Machining Operation Through Operational Modal Analysis. *International Journal of Machine Tools and Manufacture*, 49(12-13), 947-957, 0890-6955.